Scientific Research Publishing

Advances in Microbiology, 2026, 16(9), 405-423
https://www.scirp.org/journal/aim
ISSN Online: 2165-3410
ISSN Print: 2165-3402

In Silico Structural and Functional Analysis of Azo Dye Degrading Enzymes in *Lentinus* sp.

Anshu Mathur, Shalja Verma, Pravindra Kumar, Rajesh Pratap Singh, Ramasare Prasad*

Department of Biosciences and Bioengineering, Indian Institute of Technology Roorkee, Roorkee, India
Email: *ramasare.prasad@bt.iitr.ac.in

How to cite this paper: Mathur, A., Verma, S., Kumar, P., Singh, R.P. and Prasad, R. (2026) *In Silico* Structural and Functional Analysis of Azo Dye Degrading Enzymes in *Lentinus* sp. *Advances in Microbiology*, **16**, 405-423.
https://doi.org/10.4236/aim.2026.169023

Received: July 29, 2026
Accepted: September 15, 2026
Published: September 18, 2026

Abstract

Structural and functional evaluation of azo dye degrading enzymes were undertaken employing *in silico* analysis. 3D structure models for laccase (Q5EBY5) and hemeperoxidase (A0A1Q3E2I9) from the *Lentinus* sp. was generated using AlphaFold. Molecular docking was performed with AutoDock software for binding energy calculation, after identification of active site residues based on literature. Further, molecular dynamics simulation analysis was performed to evaluate the consistent binding of the dye molecules at the active site of the proteins. Molecular docking analysis revealed significant binding of three azo dyes, Amido Black 10B, Reactive Blue160, and Reactive Black 5 at the catalytic site of laccase (Q5EBY5) with significant binding energies of −7.6 kcal/mol, −7.4 kcal/mol and −6.9 kcal/mol respectively indicating Q5EBY5 laccase as the competent enzyme for remediation of dyes. Further heme peroxidase (A0A1Q3E2I9) had shown higher negative binding energy of −7.7 kcal/mol, −6.4 kcal/mol for Amido Black 10B, Reactive Black 5, respectively. The number of hydrogen bonds in both the complexes between the protein and the ligand were consistent during the simulation and revealed effective interactions.

Keywords

Fungus, Biodegradation, Homology Modelling, Molecular Docking, Textile Dyes

1. Introduction

The discharge from the textile industry is the leading contributor to water pollution, generating substantial volumes of wastewater to natural bodies like rivers and lakes, thereby posing the environmental challenge [1]. Globally, approximately 10,000 dyes and pigments are produced annually, amounting to about 0.7 million tons of synthetic dyes [2]. A prominent subset within this spectrum com-

prises azo dyes, characterized by their extensive diversity and prevalence in textile applications, accompanied by inherent challenges such as recalcitrance, limited biodegradability, and enduring presence in the environment [3]. Azo dyes, consisting of the azo bonds, exhibit remarkable stability across a broad spectrum of pH, temperature and various light exposure conditions [4]. Molecular docking serves as a pivotal tool in bioremediation strategies, facilitating the prediction of various parameters such as ligand-protein interactions, theoretical mechanisms, and toxicity. This enables a productive technology transfer to real-time setup [5]. Its application extends to the prediction and screening of pollutants for bioremediation through enzymatic systems [6]. Utilizing *in silico* approach, it can forecast the chemical nature of contaminants, propose novel xenobiotics biodegradation pathways and identify microorganisms capable of biotransformation [7] [8]. The proposed approach advocates a combination of dry lab *in silico* analysis followed by experimental confirmation as a time and cost effective strategy. This is particularly significant due to increasing levels of xenobiotics and employing promising approaches for remediation purposes.

2. Materials and Methods

2.1. Dyes and Chemicals

Table 1. Details of azo dyes used.

Azo dyes	PubChem CID	Chemical formula	Chemical structure
Amido Black 10B	135442942	$C_{22}H_{14}N_6Na_2O_9S_2$	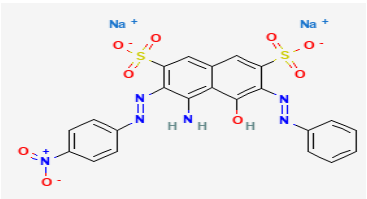
Reactive Black 5	135442967	$C_{26}H_{21}N_5Na_4O_{19}S_6$	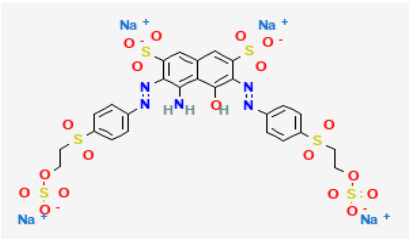
Reactive Blue 160	9577218	$C_{38}H_{23}Cl_2N_{14}Na_5O_{18}S_5$	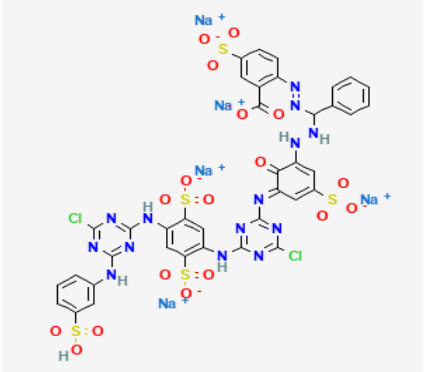

The dyes used in the study consist of Amido Black 10B (AB10B), Reactive Black 5 (RB5), Reactive Blue 160 (RB160). The information concerning the azo dyes, including their molecular formula and structure, is illustrated in Table 1.

2.2. Phylogenetic Analysis

The pair-wise sequence alignment of laccase (uniport id: Q5EBY5) with Iron permease FTR1, Cu-oxidase-domain-containing protein, Solute carrier family 40 protein, Glyco_hydro_79C domain-containing protein and several uncharacterized proteins, and heme peroxidase (uniport id: A0A1Q3E2I9) from *Lentinula edodes* was performed by BLAST analysis using a non-redundant sequence database. The top 10 hits were selected and the multiple-sequence alignment of these sequences was performed using Clustal Omega. The phylogenetic tree from multiple sequence alignment was generated to deduce the evolutionary relationship between the high similarity sequences [9] [10].

2.3. Protein Network Analysis

Protein network analysis was performed for laccase (uniport id: Q5EBY5) and heme peroxidase (uniport id: A0A1Q3E2I9) using STRING protein-protein interaction database by selecting *Lentinus tigrinus* and *Lentinula edodes* as organisms respectively. The proteins found to be interacting were evaluated for their functional association with the laccase and heme peroxidase.

2.4. Structure Modelling and Ramachandran Analysis

The protein structure was predicted by using Alpha Fold (https://colab.research.google.com/github/sokrypton/ColabFold/blob/main/AlphaFold2.ipynb) developed by DeepMind and the quality of the model was evaluated by generating the Ramachandran plot using Discovery Studio software. The quality of the structure was evaluated based on the number of residues in the favorable region of the Ramachandran Plot.

2.5. Grid Preparation and Molecular Docking of Ligands

The modeled structure of laccase (Q5EBY5) and heme peroxidase (A0A1Q3E2I9) were used for molecular docking with the dye molecules including Amido Black 10B, Reactive Black 5, and Reactive Blue 160. The 3D structures of the dye molecules were prepared using an online smile translator. Molecular docking was performed using AutoDock tools 1.5.6 version using search parameters of Lamarckian GA algorithm 4.2. The grid box dimensions considered were center X = −13.65, center Y = −4.18, and center Z = −5.79 and the grid size was X = 23.62, Y = 23.55, and Z = 28.73 for laccase (Q5EBY5) and center X = −2.76, center Y = −1.18, and center Z = 26.41 and the grid size was X = 28.6, Y = 29.32, ad Z = 32.49 for heme peroxidase (A0A1Q3E2I9). The genetic algorithm was used as search parameters including the number of GA runs of 10. The clustering of docked conformations was done using default RMSD tolerance of 2.0 Å. The proteins were

prepared for docking by polar hydrogen addition, merging of non-polar hydrogens and addition of Kollman charges. The high negative binding energy of docking and the number of hydrogen bond interactions at the active site of the enzyme were considered for the evaluation of the best binding pose [11]-[13].

Table 2. Details of proteins interacting with laccase Q5EBY5.

Accession No.	Proteins
A0A5C2S0T8	Iron permease FTR1
A0A5C2S1A8	Cu-oxidase-domain-containing protein
A0A5C2S2R5	Solute carrier family 40 protein
A0A5C2SSW2	Glyco_hydro_79C domain-containing protein
A0A5C2SIH4	uncharacterized proteins
A0A5C2SWJ8	uncharacterized proteins

2.6. Molecular Dynamic Simulation

The complexes of protein-dye molecules having high negative binding energy were considered for MD simulation for a duration of 100 ns. The ligands topologies were made using CHARMM General Force Field online server. The protein topology was made using CHARMM36 force field. The systems were solvated in dodecahedron box using Simple Point Charge water model and ions were added to neutralize the systems. The energy minimization was performed keeping maximum force limit of 10 kJ/mol. The equilibrations at number of atom pressure temperature and number of atom volume temperature at 300 K and 1 bar pressure for a duration of 100 ps each were performed for all the systems. Lastly, the systems were exposed to molecular dynamic run of 100 ns. The analysis of simulation runs was performed by considering the variations in Root Mean Square Deviation (RMSD), Root Mean Square Fluctuation (RMSF), Radius of gyration (Rg) and number of hydrogen bonds formed at each picosecond during the simulation trajectory [14].

3. Results and Discussion

3.1. *In Silico* Analysis of *Lentinus laccase and* Heme Peroxidase

The three-dimensional structure of the *Lentinus* sp. laccase and heme peroxidase were modelled using AlphaFold. Docking analysis serves as a valuable tool for investigating the interaction between proteins and ligands to elucidate the formation of stable docked complexes. This approach is instrumental in exploring both the binding and would also enable in deciphering the mechanistics of enzyme derived catalysis [14] [15].

3.2. Sequence Based Alignment and Phylogenetic Analysis of Laccase

Sequence based alignment of laccase of *Lentinus* (Uniprot ID: Q5EBY5) showed high sequence identity of 87.93% with laccase of *Polyporus brumalis* 82.54% with

laccase of *Ganoderma lucidum* and 82.72% with laccase of *Ganoderma weberianum*. Further multiple sequence alignment followed by phylogenetic analysis revealed close evolutionary affiliation of laccase of *Lentinus tigrinus* with *Polyporus brumalis* (ABN13591.1), *Cerioporus squamosus* (KAI0699344.1), *Ganoderma lucidum* (AHA83584.1) while the considered laccase is relatively less evolutionarily related with *Ganoderma weberianum* (ANA53145.1) and multiple sequence alignment analysis of laccase showed 100% similarity with *Lentinus* (Figure 1(a), Figure 1(b)).

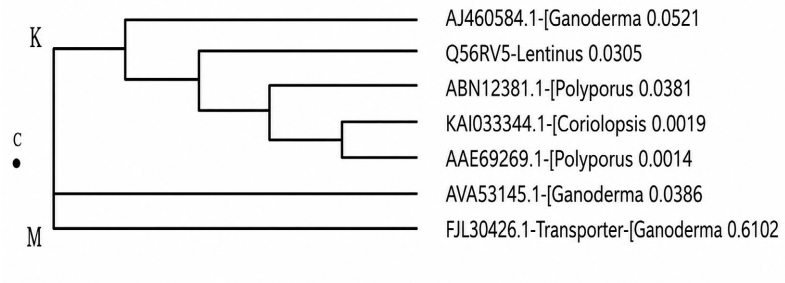

(a)

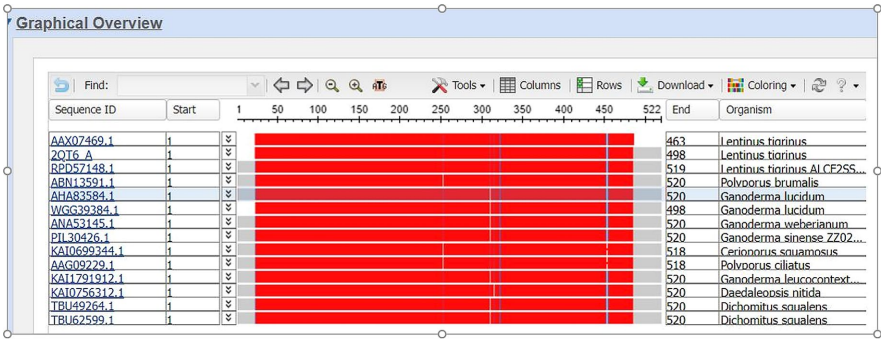

(b)

Figure 1. Phylogenetic tree (a) and multiple sequence alignment (b) analysis of laccase (Q5EBY5).

3.3. Protein-Protein Interaction Network Analysis and Structural Modeling Analysis

Network analysis of Laccase of *Lentinus* (Uniprot ID: Q5EBY5) displayed close interaction of laccase (Figure 2) with Iron permease FTR1 (A0A5C2S0T8), Cu-oxidase-domain-containing protein (A0A5C2S1A8), Solute carrier family 40 protein (A0A5C2S2R5), Glyco_hydro_79C domain-containing protein (A0A5C2SSW2) and several uncharacterized proteins (A0A5C2SIH4, A0A5C2SWJ8) (Table 2).

The Ramachandran plot analysis denoted most of the residues in favorable region explaining the high accuracy of the structure (Figure 3(a)). *In silico* analyses illustrate the enzymatic capability of *Lentinus* sp. laccase in mitigating diazo dyes through the formation of hydrogen bonds. The 3D structure of laccase (Uniprot ID: Q5EBY5) was modelled using Alpha Fold which is an AI based high accuracy protein structure prediction tool (Figure 3(b)).

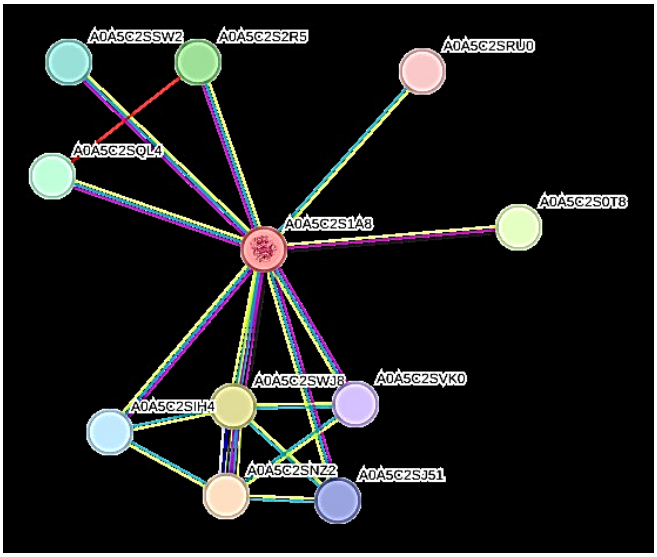

Figure 2. String network of proteins interacting with laccase (Red).

Table 3. Structural and catalytic features of laccase and heme peroxidase used for molecular docking.

Enzyme	Catalytic site basis	Docking region	Catalytic residues
Laccase (Q5EBY5)	Annotated copper-binding center	Grid box encompassing the catalytic center	Gly101, Val402, and Gln441
Heme peroxidase (A0A1Q3E2I9)	Annotated heme catalytic region	Grid box encompassing catalytic region	Arg980, Ile803

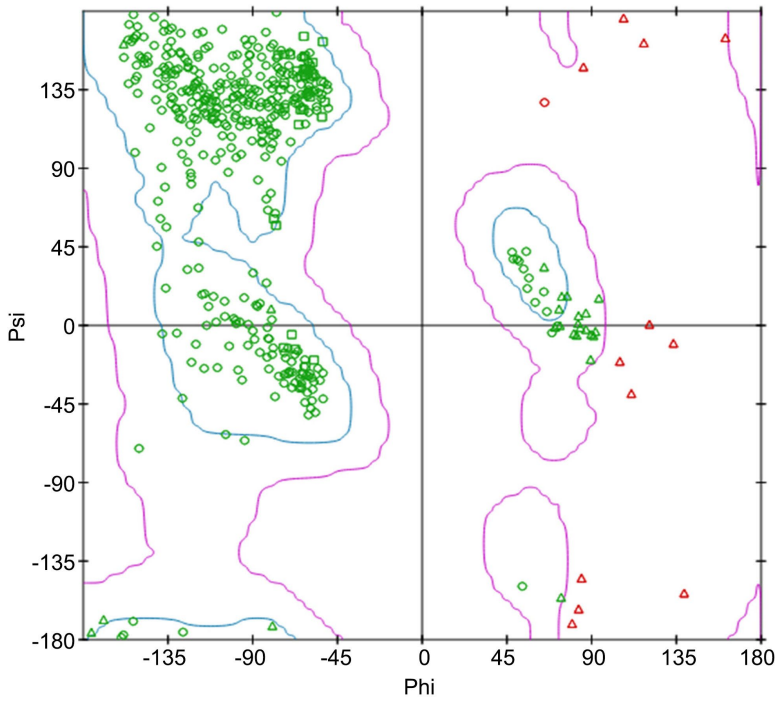

(a)

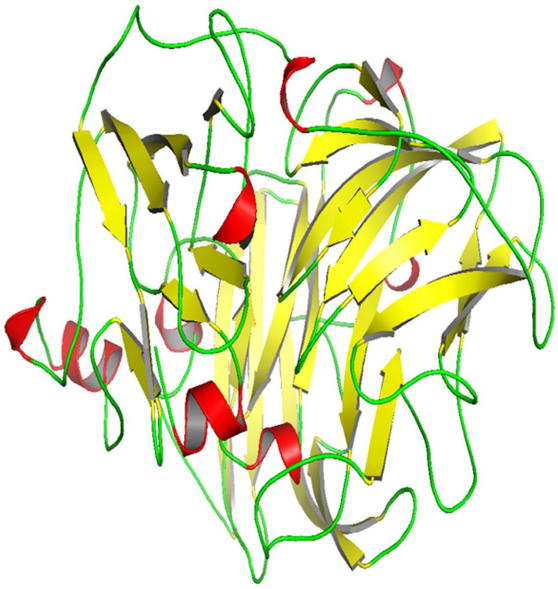

(b)

Figure 3. Ramachandran Plot (a) and modeled structure (b) of Q5EBY5 laccase of *Lentinus*.

3.4. Molecular Docking Analysis of Laccase

Molecular docking analysis revealed significant binding of three azo dyes, Amido black 10B (AB10B), Reactive Black 5 (RB5) and Reactive blue 160 (RB160), at the catalytic site of laccase (Q5EBY5) with significant binding energies of −7.6 kcal/mol, −6.9 kcal/mol and −7.4 kcal/mol respectively. Further interaction analysis revealed that Amido black 10B formed 3 hydrogen bonds with Gly101, Val402, and Gln441 (**Figure 4(a)**, **Figure 4(b)**) [16]-[18]. Additionally, these analyses indicate a slight shift in the enzyme's conformational state due to laccase-azo dyes interaction. These findings encourage the refinement of technologies tailored for synthetic dye treatment.

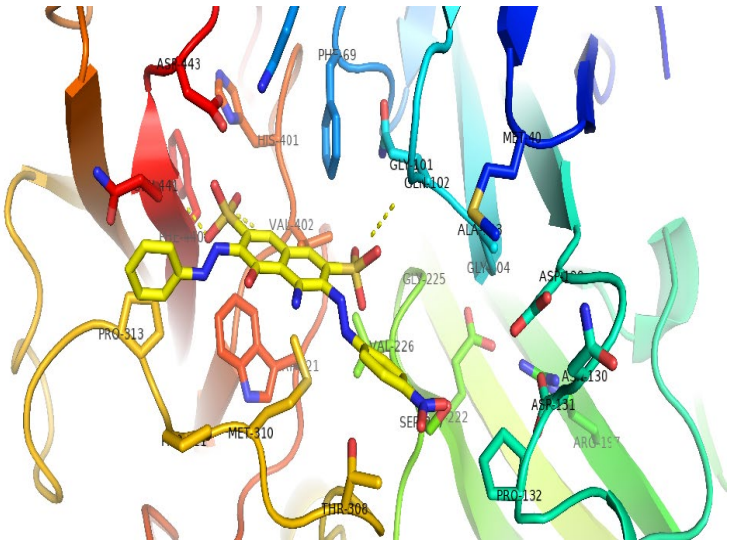

(a)

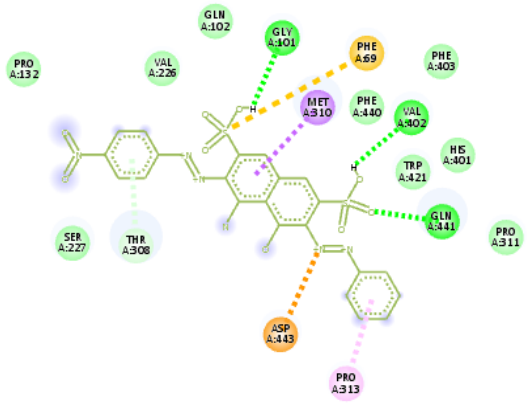
GLN A:102
GLY A:101
PHE A:69
PHE A:403
PRO A:132
VAL A:226
MET A:310
PHE A:440
VAL A:402
HIS A:401
TRP A:421
GLN A:441
PRO A:311
SER A:227
THR A:308
ASP A:443
PRO A:313

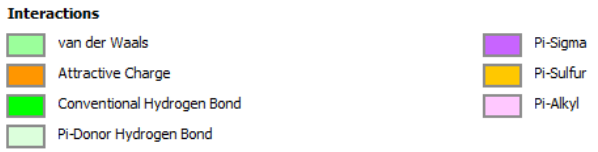
Interactions
van der Waals
Attractive Charge
Conventional Hydrogen Bond
Pi-Donor Hydrogen Bond
Pi-Sigma
Pi-Sulfur
Pi-Alkyl

(b)

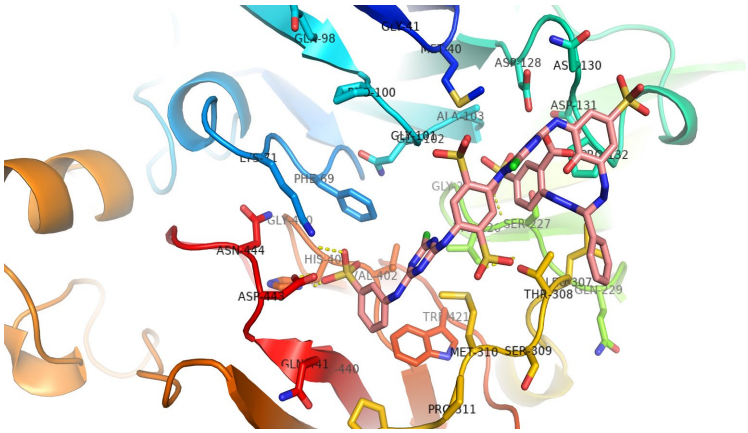
GLN-98
ASN-128
ASP-130
ASP-131
ALA-103
PHE-69
SER-227
ASN-444
HIS-401
VAL-402
THR-308
TRP-421
MET-310
SER-309
PRO-311

(c)

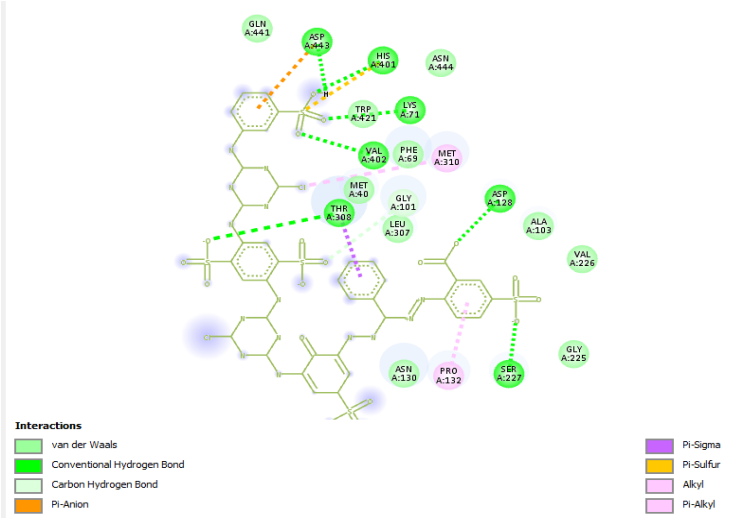
GLN A:441
ASP A:443
HIS A:401
ASN A:444
TRP A:421
LYS A:71
VAL A:402
PHE A:69
MET A:310
MET A:40
GLY A:101
THR A:308
LEU A:307
ASP A:128
ALA A:103
VAL A:226
ASN A:130
PRO A:132
SER A:227
GLY A:225
Interactions
van der Waals
Conventional Hydrogen Bond
Carbon Hydrogen Bond
Pi-Anion
Pi-Sigma
Pi-Sulfur
Alkyl
Pi-Alkyl

(d)

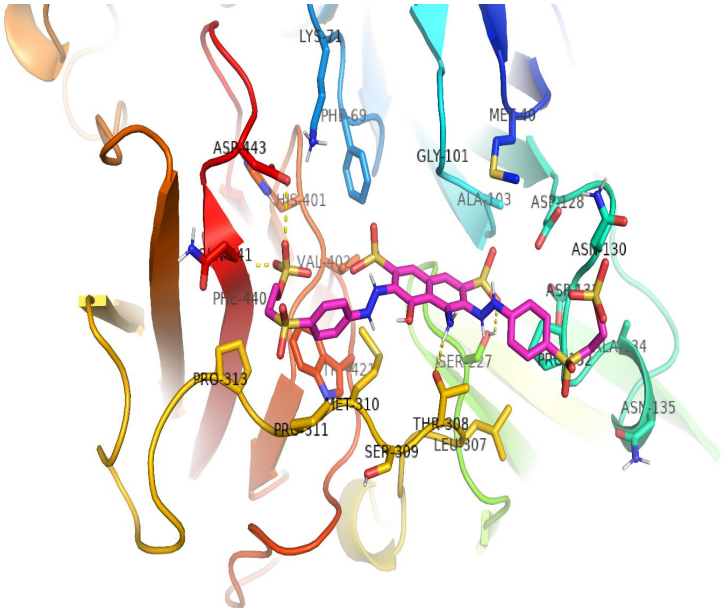

(e)

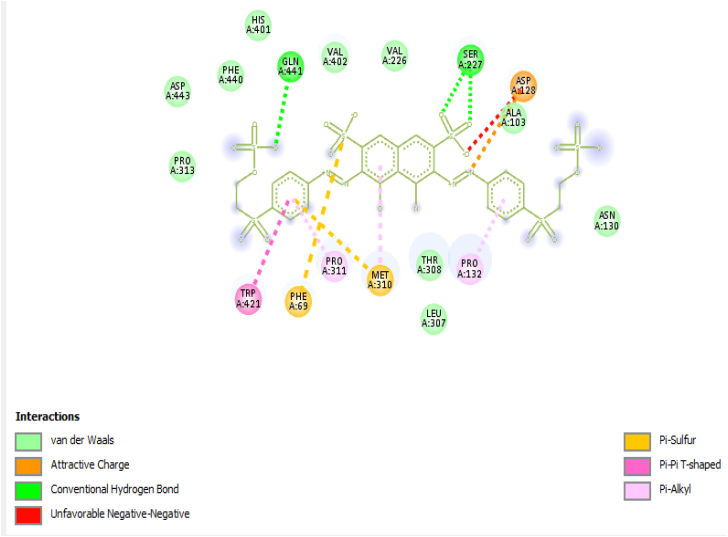

(f)

Figure 4. Docked complex of Amido black 10B with laccase (a), representation of molecular interactions in the organic residue of AB10B dye from the enzyme-ligand complex (b). Gly101, Val402, and Gln441—conventional hydrogen bonding; PHE69—Pi-sulfur; MET 310—Pi-Sigma; PRO313—Pi-Alkyl; THR306—Pi-donor hydrogen bond. Docked complex of Reactive Blue 160 with laccase (c), representation of molecular interactions in the organic residue of RB160 dye from the enzyme-ligand complex (d), LYS71, ASP443, HIS401, VAL402, THR308, AND SER227—ASP128 conventional hydrogen bonding; GLY101—carbon-hydrogen bond; MET310—Pi-Sigma; PRO132—Pi-Alkyl. Docked complex of Reactive Black 5 with laccase (e), representation of molecular interactions in the organic residue of RB5 dye from the enzyme-ligand complex (f). ASP443, PHE440, THR308, SER227—conventional hydrogen bonding; PHE69, MET310—Pi-sulfur; PRO132—Pi-Alkyl.

The interactions of Reactive black 160 had demarcated 7 hydrogen bonds with Lys71, Asp443, His401, Val402, Thr308, Ser227 and Asp128 (**Figure 4(c)**, **Figure**

4(d)).

Reactive Black 5 upon docking with laccase had resulted in 4 hydrogen bonds with Asp443, Phe440, Thr308, and Ser227 (Figure 4(e), Figure 4(f)). Thus, these indicate a potential interaction of the azo dyes with the active site of the laccase and hence further accelerate the laccase in the azo dye degradation (as shown Table 3) [14].

3.5. Molecular Dynamic Simulation of Laccase

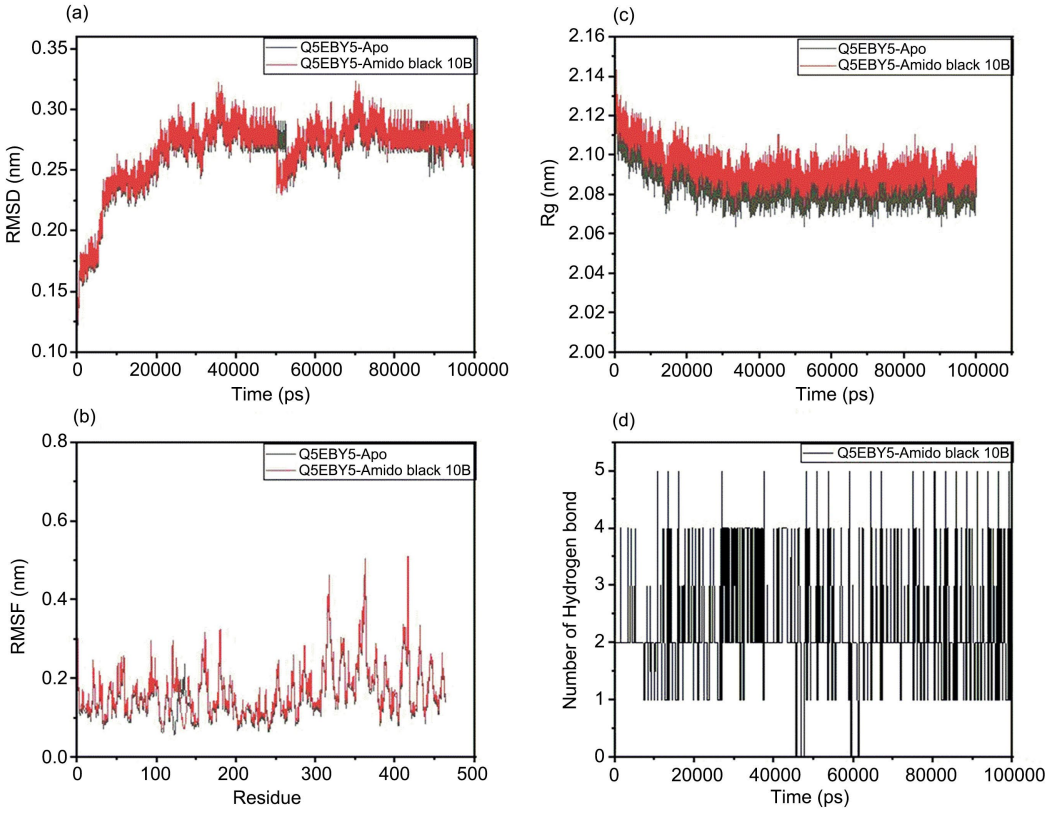

Figure 5. Analysis of MD simulation parameters for Q5EBY5-Amido black 10B complex stability, (a) Root mean square deviation (RMSD), (b) Root mean square fluctuation (RMSF), (c) Radius of gyration, (d) Hydrogen bonds analysis for Q5EBY5-Amido black 10B complex during the MD simulation trajectory of 100 ns.

Molecular dynamic simulation analysis was performed using GROMACS software for the high binding energy best docked complex of Q5EBY5 with AB10B to evaluate the stability of protein with the azo dye. Molecular dynamic simulation of apo-protein was also performed for comparative analysis. The RMSD analysis was done to assess the structural stability of the obtained complexes after virtual screening, and also to evaluate structural agreement with the crystal structure. The RMSF for each protein-ligand complex and native protein were calculated for fluctuation of the atom coordinates of the Cα to assess the flexibility of the structures, these values were evaluated with respect to the residues in the protein to estimate the motion in various residues. The RMSD values tend to converge after 20 ns and deviate from 0.12 to 0.32 nm with an average value of 0.22 nm. The

RMSD values of apo and complex forms were closer, delineating stable interaction of the ligand at the binding site (**Figure 5(a)**). The RMSF values of apo and complex showed the small fluctuation within 0.5nm in turn demarcating high stability of ligand interaction (**Figure 5(b)**). The Rg values indicated high compactness of the structure in both apo and complex forms providing evidence that the ligand binding did not impact into any major change in the structure of enzyme (**Figure 5(c)**). This study was used to assess the changes brought about by ligand binding to the protein. The consistent hydrogen bonds formed during the trajectory of 100ns apparently prove effective interaction of the AB10B at the catalytic site of the enzyme (**Figure 5(d)**). Hence, these denote Q5EBY5 laccase as effective an competent enzyme that can lead into degradation of AB10B with higher efficiency [14] [16] [19].

3.6. Sequence Based Alignment and Phylogenetic Analysis of Heme Peroxidase

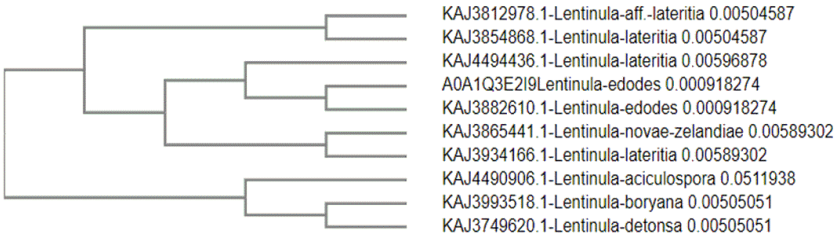

(a)

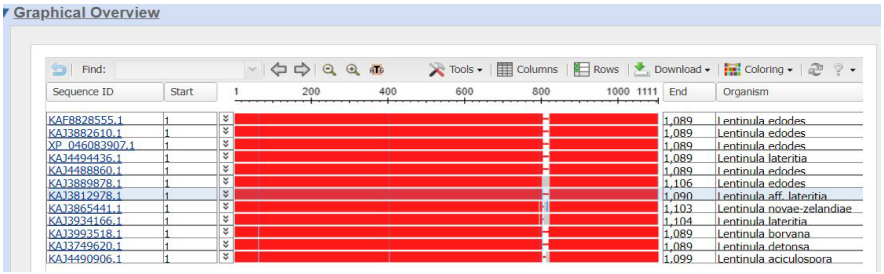

(b)

Figure 6. Phylogenetic (a) and multiple sequence alignment analysis of A0A1Q3E2I9 heme peroxidase from *Lentinula edodes* (b) and with heme peroxidase of different species.

The multiple sequence alignment followed by phylogenetic analysis of heme peroxidase from *Lentinula edodes* (A0A1Q3E2I9) revealed the effective evolutionary relationship with heme peroxidase of *Lentinula lateritia* (KAJ4494436.1). These two closely related heme peroxidases in turn showed phylogenetic relationship with heme peroxidases of *Lentinula novae-zelandiae* (*KAJ3865441.1*) and *Lentinula lateritia* (*KAJ3854868.1*). Moreover, heme peroxidases of *Lentinula aff. lateritia* (*KAJ3812978.1*), *Lentinula novae zelandiae*, *Lentinula aciculospora* (*KAJ4490906.1*), *Lentinula boryana* (*KAJ3993518.1*), and *Lentinula detonsa* (*KAJ3749620.1*) were found to have significant sequence identity and phylogenetic association with the heme peroxidase of *Lentinula edodes.* Multiple sequence

alignment analysis of heme peroxidase showed 100% similarity with *Lentinus* (Figure 6(a), Figure 6(b)).

3.7. Protein-Protein Interaction and Structural Modeling Analysis

The protein-protein network analysis revealed the closely associated proteins with that of heme peroxidase in *Lentinula edodes* (A0A1Q3E2I9) (Figure 7). The considered heme peroxidase closely interacts with two aspartate aminotransferases (A0A1Q3EHG3; A0A1Q3EG41) and one lipoxygenase (A0A1Q3ERW1). The other interacting enzymes with that of the considered heme peroxidase are given in Table 4 which include two lysophospholipase (A0A1Q3E3F4), glycoside hydrolase (A0A1Q3EQ81), protein transport protein (A0A1Q3ET19), and transmembrane protein (A0A1Q3E2D7).

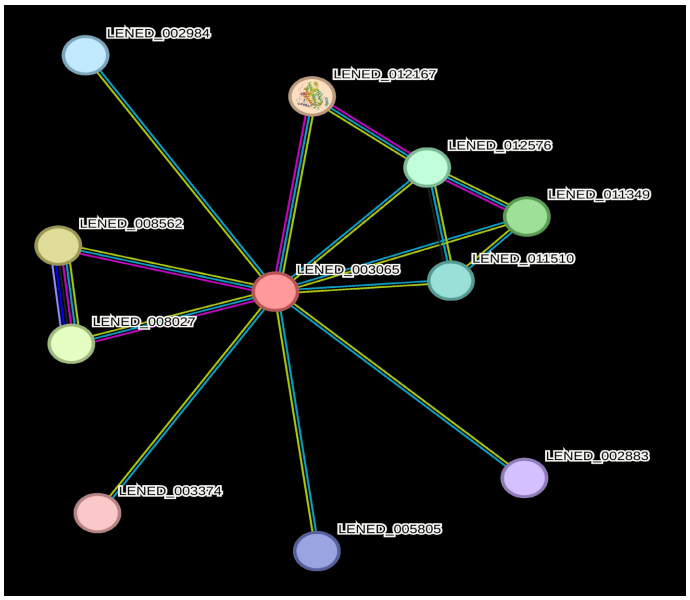

Figure 7. Protein-protein interaction network of heme peroxidase A0A1Q3E2I9 (LENED_003065) in *Lentinula edodes*.

Table 4. Details of proteins interacting with heme peroxidase A0A1Q3E2I9 (LENED_003065).

Accession No.	Proteins
LENED_002984	Transmembrane protein
LENED_012167	Lipoxygenase
LENED_012576	Protein transport protein sec16
LENED_011349	HSP20-like chaperone
LENED_011510	Glycoside hydrolase family 74 protein
LENED_003065	Heme peroxidase
LENED_008562	Aspartate aminotransferase
LENED_008027	Aspartate aminotransferase
LENED_002883	Lysophospholipase
LENED_005805	Meiotically up-regulated 190 protein

3.8. Protein Structure Modeling and Ramachandran Analysis of Heme Peroxidase

The 3D structure of heme peroxidase (A0A1Q3E2I9) was predicted by Alpha Fold and the Ramachandran analysis was performed to evaluate the modeled structure quality (Figure 8(a), Figure 8(b)). Most of the residues are in favorable regions of the Ramachandran plot proving high quality of the predicted structure [20].

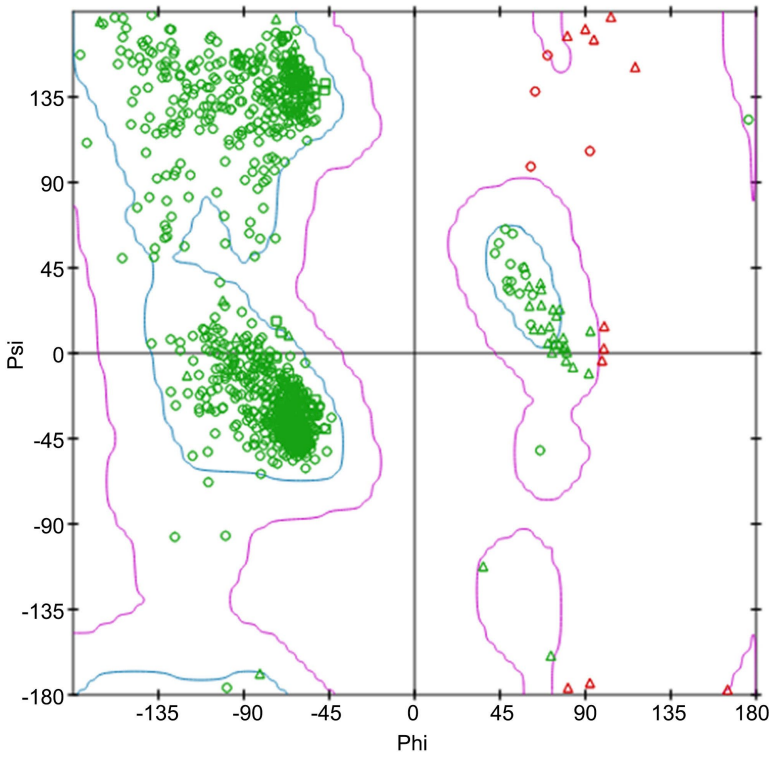

(a)

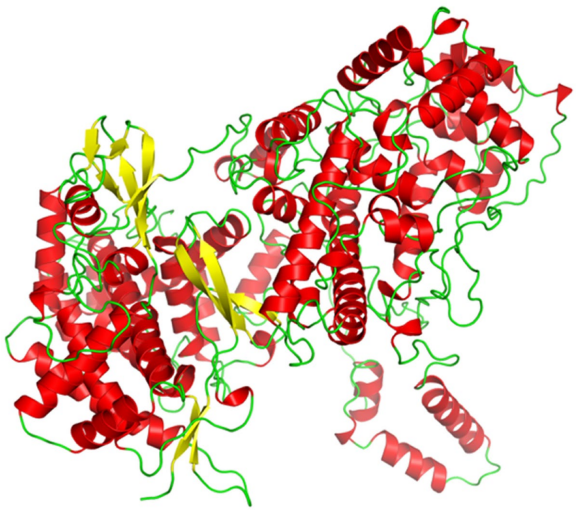

(b)

Figure 8. Ramachandran Plot (a) and modelled structure (b) of A0A1Q3E2I9 heme peroxidase of *Lentinula edodes*.

3.9. Molecular Docking Analysis of Heme Peroxidase

Molecular docking analysis of A0A1Q3E2I9 heme peroxidase of *Lentinula edodes* resulted in high negative binding energies of −7.7, −6.4 kcal/mol for Amido Black 10B form Arg980, Ile803 in conventional hydrogen bonding and Gly688-carbon-hydrogen bond (**Figure 9(a)**, **Figure 9(b)**). The interaction of RB5 shows multiple hydrogen bonds involving Tyr622, Gln685, Ile803, Thr804, Thr818, Tyr955, Asp1061, in addition Gly688, Ala821, and Lys1060 involved in carbon hydrogen bond (**Figure 9(c)**, **Figure 9(d)**). The interaction analysis showed several hydrogen bonds between heme peroxidase and AB10B and RB5. The interaction analysis of heme peroxidase with RB160 displayed unfavorable interactions of the ligand with the protein (as shown in **Table 3**) [21].

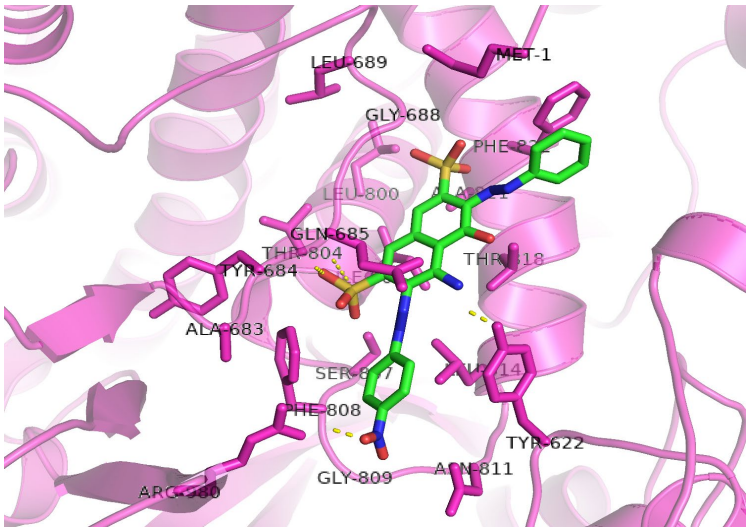

(a)

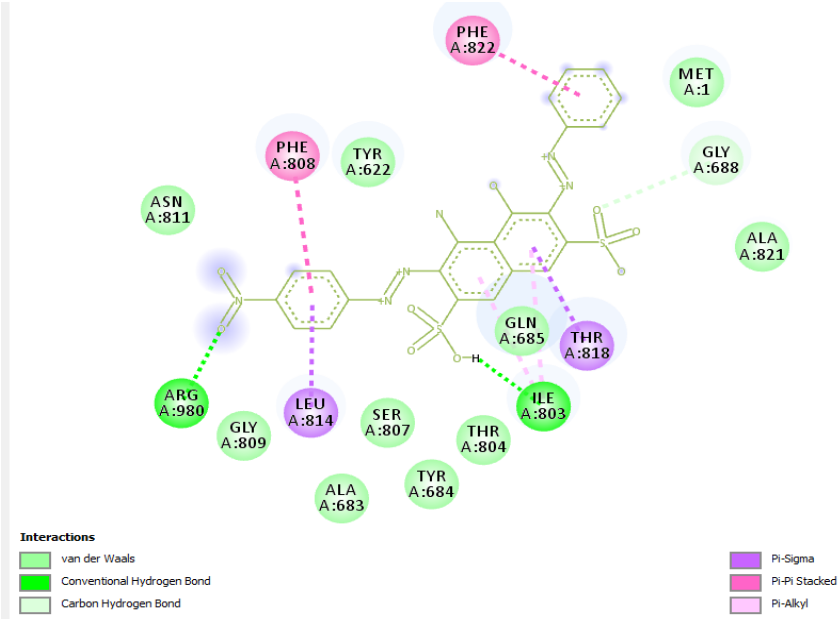

(b)

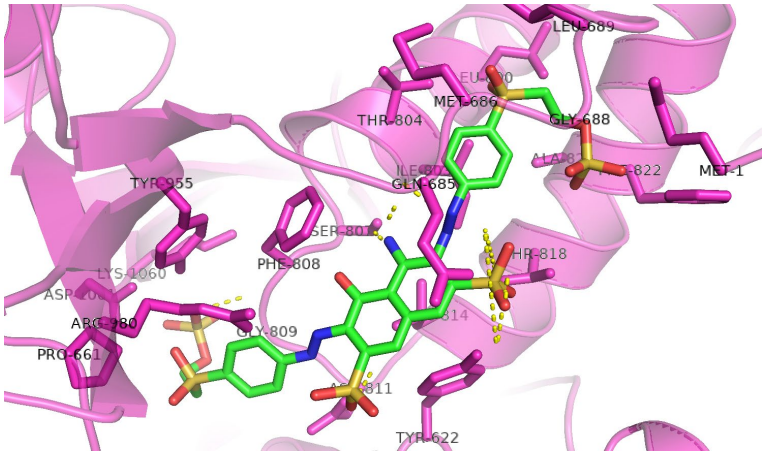

(c)

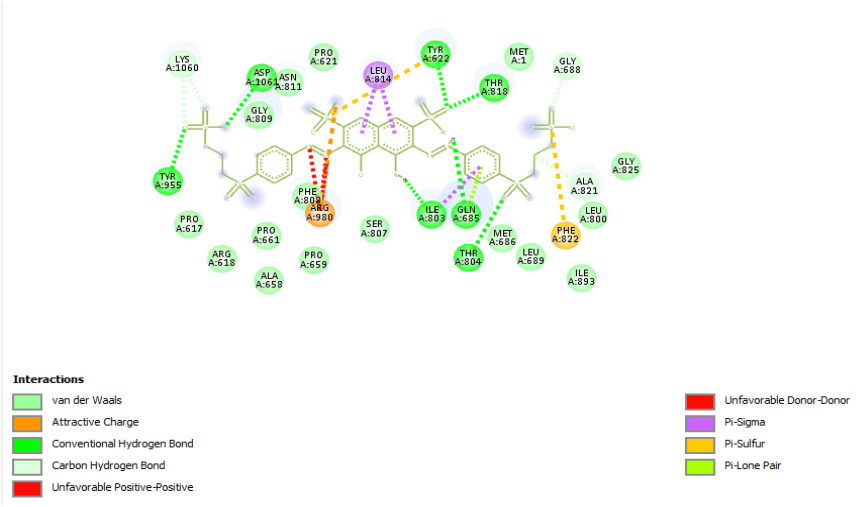

(d)

Figure 9. Docking interactions between heme peroxidase and Amido Black 10B (a), representation of molecular interactions in the organic residue of AB10B dye from the enzyme-ligand complex (b). ARG980, ILE803 conventional hydrogen bonding; GLY688—carbon-hydrogen bond; LEU814, THR818—Pi-Sigma. Docking interactions between heme peroxidase and Reactive Black 5 (c), representation of molecular interactions in the organic residue of RB5 dye from the enzyme-ligand complex (d). TYR622, GLN685, ILE803, THR804, THR818, TYR955, ASP1061—conventional hydrogen bonding; GLY688, ALA821, LYS1060—carbon-hydrogen bond; LEU814—Pi-Sigma; PHE822—Pi-Sulfur.

3.10. Molecular Dynamic Simulation of Heme Peroxidase

Molecular dynamic simulation of the apo-heme peroxidase and complexes of heme peroxidase with Amido Black 10B and Reactive Black 5 were performed. The RMSD values with respect to time of apo-protein as well as that of complexes were in the range of 0.15 to 0.5 nm with an average value of 0.3 nm during the trajectory denoting high stability of the complexes due to the least deviations in complexes (**Figure 10(a)**). Stable interaction have been observed earlier [22]. The RMSF values showed similar fluctuations in AB10B complex to that of the apo-heme peroxidase denoting relatively higher stability of the interactions compared

to the other dye RB5 (Figure 10(b)). The overall fluctuations were less than 1nm thus both the ligands did not pose any major structural change in the protein and demarcated higher stability of complexes. The Rg values of both the complexes were similar to that of the apo-protein and varied in the range of 2.80 to 3.00 nm during the simulation trajectory thus attributing high compactness of the protein during simulation period of 100 ns (Figure 10(c)). The number of hydrogen bonds calculated at each picosecond in both the complexes between the protein and the ligand were consistent during the simulation and revealed effective interactions between protein and ligand during the 100 ns simulation (Figure 10(d)).

Several structural characteristics contributing to novel structural, catalytic, and stability features have been unveiled through bioinformatics driven genome-wide analysis [23] [24].

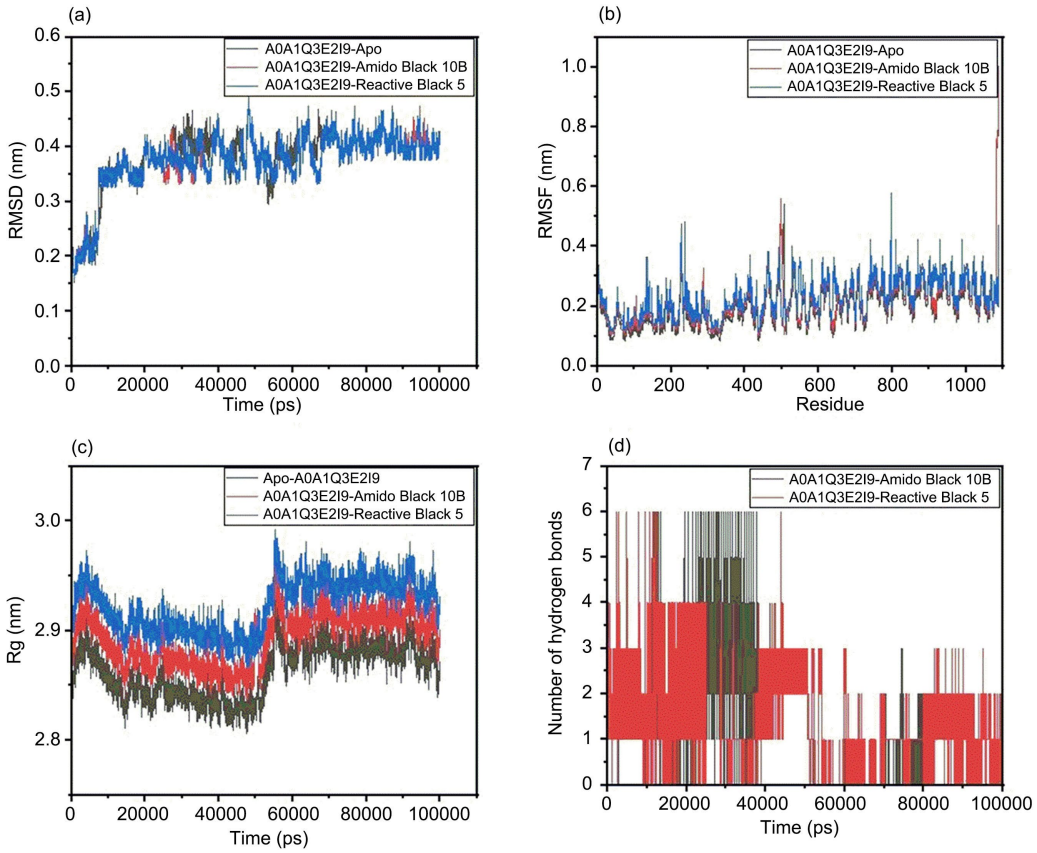

Figure 10. Analysis of MD simulation parameters for A0A1Q3E2I9-ligand complex stability, (a) RMSD, (b) RMSF, (c) Rg, (d) Number of hydrogen bonds with respect to time in A0A1Q3E2I9-ligand complexes during the trajectory period of 100 ns.

4. Conclusion

The catabolism of azo dyes denoted the pivotal enzymes involved in dye degradation mainly laccase, manganese peroxidase, lignin peroxidase, and other enzyme associated with the dye. Molecular docking analysis revealed binding of three azo dyes, AB10B, RB5, and RB160 at the catalytic site of laccase (Q5EBY5) with sig-

nificant binding energies. Laccase (Q5EBY5) effective enzyme for remediation of the dyes. In addition, heme peroxidase had also shown stable interaction with AB10B and RB5. The number of hydrogen bonds in both the complexes between the protein and the ligand were consistent during the simulation and revealed effective interactions. Thus, effective binding and significant interactions of the azo dyes with active sites illustrate the potential of the enzymes in the degradation of dyes. In our previous study, Mathur *et al.* (2024), *Lentinus squarrosulus* AF5 demonstrated efficient azo dye degradation. Chromatographic and spectroscopic analyses confirmed the transformation of the dyes and the formation of degradation products, while subsequent phytotoxicity and cytotoxicity assessments indicated substantially reduced toxicity of the metabolites. These findings established *L. squarrosulus* AF5 as a promising fungal biocatalyst for azo dye bioremediation and provided the basis for further investigation of the molecular mechanisms underlying enzyme-dye interactions and degradation. Building on this previous work, the present study further explores the potential involvement of ligninolytic enzymes through molecular docking and structural analysis. These results expand our understanding of the fungal mechanisms involved in dye degradation and serve as a catalyst for scaling up this process for the treatment of textile effluents.

Author Contributions

Anshu Mathur: Conceptualization, Investigation, Visualization, Writing-Original Draft Shalja Verma: Investigation, Validation and visualization.

Pravindra Kumar: Software, Validation.

R. Prasad: Supervision, Writing-Review & Editing.

R. P. Singh: Supervision, Visualization, Writing-Review & Editing.

Acknowledgements

The author AM gratefully acknowledge Department of Biotechnology, Govt. of India for the financial assistantship and the Institute Instrument Center, IIT Roorkee for the instrumentation facility.

Conflicts of Interest

The authors declare that they have no conflict of interest.

References

[1] Hassan, M.M. and Carr, C.M. (2018) A Critical Review on Recent Advancements of the Removal of Reactive Dyes from Dyehouse Effluent by Ion-Exchange Adsorbents. *Chemosphere*, **209**, 201-219. https://doi.org/10.1016/j.chemosphere.2018.06.043

[2] Shah, M. (2014) Effective Treatment Systems for Azo Dye Degradation: A Joint Venture between Physico-Chemical & Microbiological Process. *International Journal of Environmental Bioremediation & Biodegradation*, **2**, 231-242.

[3] Gayathri, K., Saranraj, P., Nayak, A.K., Kesavardhini, K., Lokeshwari, B. and Cardoso, A.M. (2026) Microbial Innovations for Sustainable Wastewater Management: A Comprehensive Review of Azo Dye Bioremediation. *Sustainability*, **18**, Article No.

3041. https://doi.org/10.3390/su18063041

[4] Kamal, I.M., Abdeltawab, N.F., Ragab, Y.M., Farag, M.A. and Ramadan, M.A. (2022) Biodegradation, Decolorization, and Detoxification of Di-Azo Dye Direct Red 81 by Halotolerant, Alkali-Thermo-Tolerant Bacterial Mixed Cultures. *Microorganisms*, **10**, Article No. 994. https://doi.org/10.3390/microorganisms10050994

[5] Verma, S., Singh, A., Kumar, P. and Singla, J. (2024) *In-Silico* Characterization of a Hypothetical Protein of Sulfobacillus Sp. Hq2 for Degradation of Phthalate Diesters. *International Journal of Biological Macromolecules*, **280**, Article ID: 136006. https://doi.org/10.1016/j.ijbiomac.2024.136006

[6] Suresh, P.S., Kumar, A., Kumar, R. and Singh, V.P. (2008) *An Insilco* Approach to Bioremediation: Laccase as a Case Study. *Journal of Molecular Graphics and Modelling*, **26**, 845-849. https://doi.org/10.1016/j.jmgm.2007.05.005

[7] Sarkar, C., Jaimini, D., Shabnam, A.A. and Sarkar, C. (2012) *In-Silico* Feasibility of Novel Biodegradation Pathways For1-Naphthyl Methylcarbamate. *The Journal of Toxicological Sciences*, **4**, 89-93.

[8] Reena, Dhall, P., Kumar, R. and Kumar, A. (2014) Validation of Computationally Predicted Substrates for Laccase. *Brazilian Archives of Biology and Technology*, **57**, 803-809. https://doi.org/10.1590/s1516-8913201402239

[9] Altschul, S.F., Gish, W., Miller, W., Myers, E.W. and Lipman, D.J. (1990) Basic Local Alignment Search Tool. *Journal of Molecular Biology*, **215**, 403-410. https://doi.org/10.1016/s0022-2836(05)80360-2

[10] Coelho, G.D., Silva, M.A., de Melo Pinheiro, M.A., Nadvorny, D., Costa Amador, V. and Maia, R.T. (2024) *In Silico* and *in Vitro* Assays Suggests Congo Red Dye Degradation by a *Lentinus* sp. Laccase Enzyme. *Journal of Biomolecular Structure and Dynamics*, **42**, 3802-3813. https://doi.org/10.1080/07391102.2023.2216282

[11] Venkatachalam, C.M., Jiang, X., Oldfield, T. and Waldman, M. (2003) LigandFit: A Novel Method for the Shape-Directed Rapid Docking of Ligands to Protein Active Sites. *Journal of Molecular Graphics and Modelling*, **21**, 289-307. https://doi.org/10.1016/s1093-3263(02)00164-x

[12] Sarkar, S., Banerjee, A., Chakraborty, N., Soren, K., Chakraborty, P. and Bandopadhyay, R. (2020) Structural-Functional Analyses of Textile Dye Degrading Azoreductase, Laccase and Peroxidase: A Comparative *in Silico* Study. *Electronic Journal of Biotechnology*, **43**, 48-54. https://doi.org/10.1016/j.ejbt.2019.12.004

[13] Srinivasan, S., Sadasivam, S.K., Gunalan, S., Shanmugam, G. and Kothandan, G. (2019) Application of Docking and Active Site Analysis for Enzyme Linked Biodegradation of Textile Dyes. *Environmental Pollution*, **248**, 599-608. https://doi.org/10.1016/j.envpol.2019.02.080

[14] Pande, V., Joshi, T., Pandey, S.C., *et al.* (2022). Molecular Docking and Molecular Dynamics Simulation Approaches for Evaluation of Laccase-Mediated Biodegradation of Various Industrial Dyes. *Journal of Biomolecular Structure and Dynamics*, **40**, 12461-12471. https://doi.org/10.1080/07391102.2021.1971564

[15] Singh, A.K., Bilal, M., Iqbal, H.M.N. and Raj, A. (2021) Trends in Predictive Biodegradation for Sustainable Mitigation of Environmental Pollutants: Recent Progress and Future Outlook. *Science of the Total Environment*, **770**, Article ID: 144561. https://doi.org/10.1016/j.scitotenv.2020.144561

[16] Prasad, N.K., Vindal, V., Narayana, S.L., *et al.* (2012) *In Silico* Analysis of *Pycnoporus cinnabarinus* Laccase Active Site with Toxic Industrial Dyes. *Journal of Molecular Modeling*, **18**, 2013-2019. https://doi.org/10.1007/s00894-011-1215-0

[17] de Ruyck, J., Brysbaert, G., Blossey, R. and Lensink, M. (2016) Molecular Docking as a Popular Tool in Drug Design, an *in Silico* Travel. *Advances and Applications in Bioinformatics and Chemistry*, **9**, 1-11. https://doi.org/10.2147/aabc.s105289

[18] Coelho, G.D., Silva, K.K.S., Silva, D.P.D., Soares, J.K.N.C., Ballaminut, N. and Thomaz, D.V. (2020) Biodegradation of Synthetic Effluent Containing CI Direct Red 28 (Congo Red) by *Lentinus* sp. Laccase Leads to Low Ecotoxicity. *Current Biotechnology*, **9**, 127-133. https://doi.org/10.2174/2211550109999200720162021

[19] Almeida, P.H., Oliveira, A.C.C.D., Souza, G.P.N.D., Friedrich, J.C., Linde, G.A., Colauto, N.B., *et al.* (2018) Decolorization of Remazol Brilliant Blue R with Laccase from *Lentinus crinitus* Grown in Agro-Industrial By-Products. *Anais da Academia Brasileira de Ciências*, **90**, 3463-3473. https://doi.org/10.1590/0001-3765201820170458

[20] Badyal, S.K., Joyce, M.G., Sharp, K.H., Seward, H.E., Mewies, M., Basran, J., *et al.* (2006) Conformational Mobility in the Active Site of a Heme Peroxidase. *Journal of Biological Chemistry*, **281**, 24512-24520. https://doi.org/10.1074/jbc.m602602200

[21] Dhankhar, P., Dalal, V., Singh, N., Gurjar, B.R., Sharma, A.K. and Kumar, P. (2020) Bioremediation of Synthetic Dyes: Dye Decolorizing Peroxidases (DyPs). In: *Removal of Toxic Pollutants Through Microbiological and Tertiary Treatment*, Elsevier, 453-486. https://doi.org/10.1016/b978-0-12-821014-7.00018-6

[22] Knapp, B., Frantal, S., Cibena, M., Schreiner, W. and Bauer, P. (2011) Is an Intuitive Convergence Definition of Molecular Dynamics Simulations Solely Based on the Root Mean Square Deviation Possible? *Journal of Computational Biology*, **18**, 997-1005. https://doi.org/10.1089/cmb.2010.0237

[23] Ohm, R.A., Riley, R., Salamov, A., Min, B., Choi, I. and Grigoriev, I.V. (2014) Genomics of Wood-Degrading Fungi. *Fungal Genetics and Biology*, **72**, 82-90. https://doi.org/10.1016/j.fgb.2014.05.001

[24] Fernández-Fueyo, E., Linde, D., Almendral, D., López-Lucendo, M.F., Ruiz-Dueñas, F.J. and Martínez, A.T. (2015) Description of the First Fungal Dye-Decolorizing Peroxidase Oxidizing Manganese(II). *Applied Microbiology and Biotechnology*, **99**, 8927-8942. https://doi.org/10.1007/s00253-015-6665-3